

Investigations of casting conditions in a Two – Strand – Tundish Water Model using DPIV and PLIF-technique

A. Braun, H. Pfeifer

RWTH Aachen, Institut für Industrieofenbau und Wärmetechnik, IOB
Kopernikusstr. 16, 52074 Aachen

Abstract

The investigated multi-strand tundish distributes the steel melt from the ladles to the two moulds. Laser optical investigations were carried out at a 1:3 scaled laboratory water model of a Two-strand-tundish. The steel tundish has a capacity of 69 t. To illustrate the influence of different casting conditions on the flow field and the mixing process in the tundish Digital Particle Image Velocimetry (DPIV) and Planar Laser Induced Fluorescence (PLIF) are used. The operation of one of the moulds can be interrupted due to some limitations of process in the continuous casting. An example of these limitations is the clogging of the submerged entry nozzle (SEN). Since the Two-strand-tundish has to guarantee perfect casting conditions at the unaffected mould, the conditions at the inlet have to be adapted. The mass flow rate must be reduced and therefore the casting time increases. The Froude criterion is kept to determine the volumetric flow rate for the water model. The presented investigations show that different casting conditions have a large influence on the flow phenomena inside the tundish. The interruption of the casting process at one of the moulds leads to a change of the characteristic flow structure and on the mixing process of the fluid

Introduction

Continuous casting plants in steel mills have to process liquid steel into the requested shapes such as slabs and billets. These plants link the discontinuous process of ladle metallurgy with the continuous casting process [9,10]. Advantages of the continuous process are a higher yield and the possibility of automation. The steel flow, temperature and concentration distribution of non-metallic particles (Al_2O_3 or SiO_2) within ladle, tundish and moulds are of decisive importance for the quality of steel [5,7]. The tundish regulates the flow from the ladle to the mould. It serves as a buffer and supports the particle separation. The investigated tundish is characterized by a molten steel mass flow of more than 300 t/h. It feeds simultaneously two moulds for the production of steel slabs with a 1600 mm x 63 mm cross section. The maximum capacity of the T-shaped-tundish is 69 t. The characteristics of the flow in a tundish include jet spreading, jet impingement on the wall, wall jets and decrease of turbulence intensity in the region far from the jet. Concerning the tundish two kinds of flow conditions are defined:

During **undisturbed steady-state casting** the mass of steel in the tundish is constant. In this case, the inflow \dot{m}_{sh} through the shroud (sh) is equal to the sum of both outlets $\dot{m}_{\text{SEN,A}} + \dot{m}_{\text{SEN,B}}$ through the Submerged Entry Nozzles (SENs) into the moulds. Thus, the steel level in the tundish is constant.

The expression **disturbed steady-state casting** means that just one of the outflows of the Two-strand-tundish is in operation. In the continuous casting process a disturbance can lead to rapid switching off of one of the strand moulds. In spite of such disturbances the process must be ensured to work continuously at the further casting mould. The mass flow from the ladle must be

29.2

reduced and adapted on the new casting conditions. Thus, the residence time of the melt becomes larger both in the tundish and in the ladle. With the continuing casting disturbance, technical measures become necessary to prevent a premature complete casting interruption and to maintain acceptable casting conditions. Such a measure is for example the external heating of the melt in the tundish with electric arcs.

A fluidic and thermo-mechanical investigation of the melt flow in a steel mill is nearly impossible due to the high temperatures and a lack of optical accessibility. In order to determine the fluid flow structure and the mixing process physical simulations were carried out consideration of the similarity numbers.

Test Setup

The laser optical measurements were carried out at a 1:3 scaled water model [1]. The water model tundish can be operated either in an opened or closed circuit. If the closed circuit is used, the water will flow out of the tundish into the SEN's (Submerged Entry Nozzles), through the pump and flow meter and shroud back into the tundish. This operation is used during the calibration of the PLIF system. When operating in an open circuit, fresh water is supplied to the tundish, while the contaminated water is pumped out of the tundish into the discharge. The operation state and the filling level H remains constant. This operation mode is used after the calibration has been finished and the mixing process is simulated. Figure 1 and Table 1 give an overview about the geometrical dimensions and the used nomenclature.

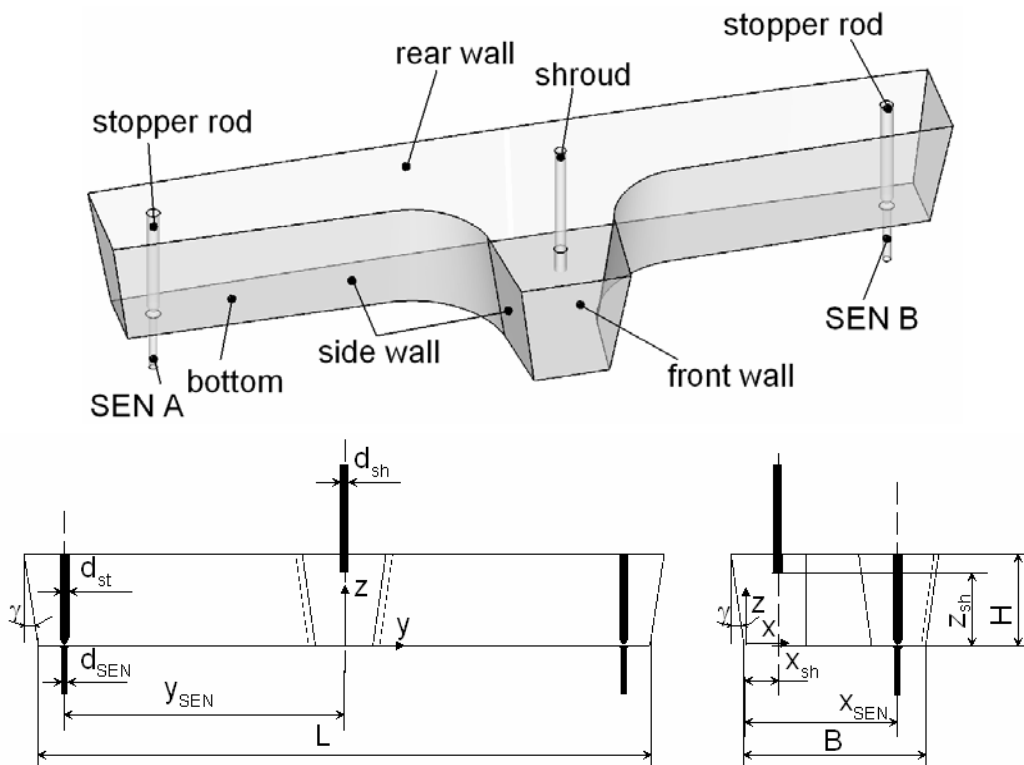


Figure 1: Geometrical description of the 69 t-Two-Strand-Tundish

To transfer results of measurements from a model to the original tundish, apart from the geometric similarity, the fluid-dynamic similarity must be considered as well. The observance of the Re- and Fr-similarity is determining [3]. The Re-number describes the dynamic flow behaviour by the ratio of inert to friction forces and is characteristic for the location and extension of flow structures. The Fr-number is a criterion for flows influenced by gravitational force like free surface or buoyancy driven flows.

Table 1: Dimensions of the original tundish and the water model

| Name | Abbr. | Two-Strand Tundish | |
|-------------------------------|-----------------------|--------------------|----------------------------|
| | | Original | Water Model (Scale 1:3) |
| tundish volume | V in m ³ | 9.639 | 0.357 |
| tundish length | L in m | 8.013 | 2.671 |
| tundish width | B in m | 2.271 | 0.757 |
| steel level | H in m | 1.14 | 0.38 |
| inclination of the side walls | γ in ° | 8 | 8 |
| position of the shroud | x _{SR} in m | 0.42 | 0.14 |
| height between bottom–shroud | z _{SR} in m | 0.912 | 0.304 |
| diameter of the shroud | d _{SR} in m | 0.12 | 0.040 |
| position of the SEN | x _{SEN} in m | 1.92 | 0.64 |
| position of the SEN | y _{SEN} in m | 3.825 | 1.275 |
| diameter of the SEN | d _{SEN} in m | 0.090 | 0.030 |
| diameter of the stopper rod | d _{ST} in m | 0.123 | 0.041 |

In a reduced 1:3 scaled water model the Reynolds and the Froude number cannot be satisfied simultaneously. Therefore and because high Reynolds numbers lead to strong surface waves and a formation of air bubbles, that affect the DPIV-measurements, the Froude number is regarded. Former investigations show that in geometrically similar models the characteristic flow structures for $Re > Re_{critical}$ remain unchanged [11]. The fluid-dynamic data are given in Table 2.

Table 2: Comparison of data: original tundish and water model

| Name | Abbr. | Two-Strand Tundish | |
|----------------------------|-----------------------------|---------------------|----------------------------|
| | | Original | Water Model (Scale 1:3) |
| density | ρ in kg/m ³ | 7038 | 998.2 |
| viscosity | ν in m ² /s | $8.7 \cdot 10^{-7}$ | $10.1 \cdot 10^{-7}$ |
| volume flow rate in l/s | \dot{V}_{sh} in l/s | 9.6 | 0.62 |
| mean velocity inlet region | \bar{u} in m/s | 0.0105 | 0.006 |
| theoretical residence time | \bar{t} in s | 1027 | 580 |
| Froude number | Fr | $2.2 \cdot 10^{-6}$ | $2.2 \cdot 10^{-6}$ |
| Reynolds number | Re | 16900 | 2600 |

The test facility is equipped with a combination of a frequency converter and a centrifugal pump. The volume flow rate is measured with a magnetic inductive flowmeter.

The information obtained at physical models can be used to validate further numerical simulations. If the comparison between physical and numerical simulation shows a good agreement, the numerical simulation can be transferred to the flow of liquid steel which is actually the matter of interest as the next step.

Measurement Techniques

The fundamental DPIV test set-up is illustrated in figure 4. DPIV is a non-intrusive, laser-optical method to record time-dependent velocity fields [12].

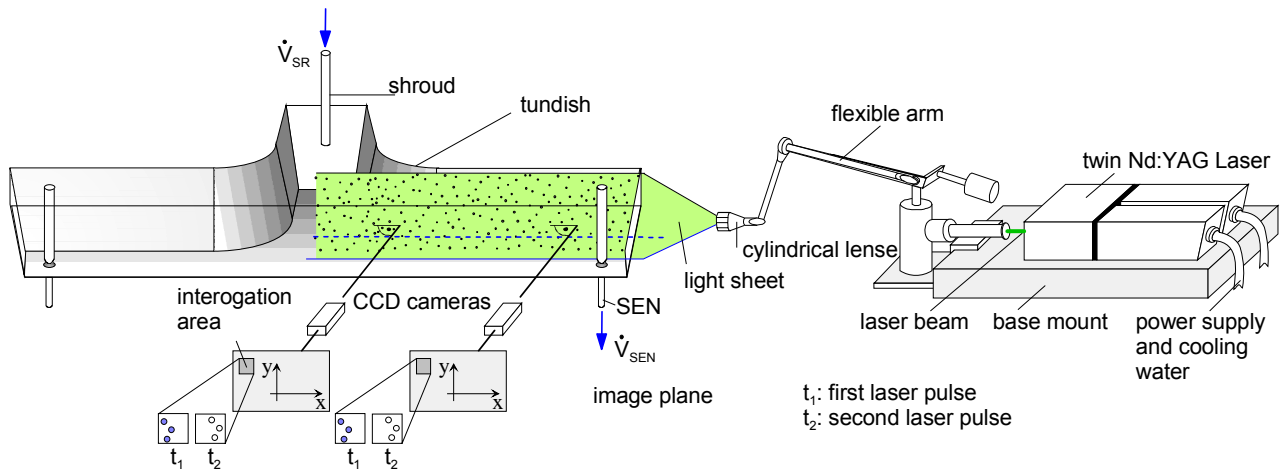


Figure 2: Experimental set-up for 2D-DPIV/PLIF measurements

It is based on the imaging, tracking and recording of small particle patterns, which are added to the flow and move along together with the flow and thereby retain their individuality. The particles are illuminated inside a thin laser-light sheet at defined intervals of time. The reflected light is observed perpendicular to the light sheet plane by CCD cameras. From the displacement of a particle pattern during a known time interval Δt_{DPIV} at a location (i,j) within a specified plane, it is possible to determine the local velocity vector and accordingly, the two-dimensional velocity field. The basic-condition is that the particle velocity corresponds to the local flow velocity. The DPIV facility consists of two pulsed Nd:YAG lasers. Table 2 indicates the most important technical data. A more detailed description of the facilities can be found in [1, 8, 10].

Table 3: Technical data of the DPIV and PLIF-System

| | | |
|--|--|---|
| Double cavity Nd:YAG-laser system with flexible arm (1.80 m) | wave length λ repetition rate f pulse energy E_{max} pulse duration t min. time between pulses $\Delta t_{DPIV, min}$ Thickness of light sheet Δy_0 | 532 nm 15 Hz 140 mJ 4.3 ns 2000 μ s 2 mm |
| Two Kodak Megaplug ES 1.0 cameras | resolution digital output repetition rate f (double exposure) | 1008 x 1018 Pixel 8 bit 1 - 3 Hz |
| PLIF tracer: Rhodamine 6G | chemical formula absorption spectrum $\lambda_{rh,a}$ emission spectrum $\lambda_{rh,e}$ solubility s_{rh} density ρ_{rh} pH factor pH_{rh} | $C_{27}H_{28}N_2O_3HCl$ 460-570 nm, $\lambda_{max} = 530$ nm 540-640 nm, $\lambda_{max} = 560$ nm 30 g/l _w at 20°C 1.28 g/cm ³ 6.5 |

The concentration field inside the tundish is determined using the Laser Induced Fluorescence. PLIF uses the frequency shift of the light emitted by fluorescent substances to measure scalar quantities in fluids such as the concentration or temperature. The fluorescence signal is recorded by CCD (Charged Couple Device) cameras, which are equipped with monochromatic filters to separate the fluorescence signal from the excitation light. PLIF is a non-intrusive in-situ-measurement technique with a high temporal and/or spatial resolution. The DPIV measurement system is converted into a PLIF system by using different optical filters to detect the emitted light of the fluorescent dye. These tracers should have a high quantum yield, must be adapted to the light source and must be soluble in water. The used rhodamine 6G solution meets best to these demands.

The laser light of the energy E_0 and intensity I_0 , respectively, induces a decreased intensity I_E inside the laser light sheet depends on the local position. The detected fluorescence intensity I_D measured by the CCD camera at an arbitrary pixel element P can be assigned to the local concentration C [2,4].

The Calibration process of the PLIF system is described in detail in [6]. At the start of calibration, the test set-up with fresh water is operated in a closed circuit ($c_{rh} = 0 \%$). A certain amount of rhodamine 6G is dissolved in 100 ml water and is added in steps of 10 %. Subsequently, the tundish volume is stirred until a homogeneous concentration is reached. After the stirring time each of the CCD camera takes ten images whereby the stored grey-tone values are averaged for each pixel. This way, the pulse to pulse fluctuations of the emitted laser power which are to be found within the range of 4 % can be compensated. The influence of the intensity variation is then reduced to 1.3 % ($4 \%/ \sqrt{10}$). At the end of the calibration, the maximum concentration in the water model tundish is $c_{rh} = 100 \%$ ($C_{rh,max} = 50 \mu\text{g}_{rh}/l_w$). If the concentration further increases, non-linear saturation effects will appear due to quenching. When using rhodamine 6G as fluorescent dye with a maximum concentration of $C_{rh,max} = 50 \mu\text{g}_{rh}/l_w$, non-linear effects can be excluded. Due to the calibration procedure of the PLIF system, the optical, geometrical and physical parameters do not have to be determined.

When starting the measurements, the piping is switched from the closed to the open circuit and fresh water is supplied to the tundish model. From this time on, the temporal decrease of the Rhodamine 6G concentration is measured.

Results of the physical simulations

Figure 3 shows results of 2D-DPIV measurements for isothermal casting conditions. The size of the interrogation area is 64×64 pixels with 75 % overlap. The velocity magnitude is represented by the colourmap. The jet entering the tundish through the shroud impinges on the bottom of the Two-strand-tundish and flows towards the front wall ($x/B = 0$) and the rear wall ($x/B = 1$). On the rear wall the flow is diverted towards the outlets. Former investigations [1] already presented that in the outlet region a dominant vortex structure arises. This vortex transports fluid on its surface to the outlet. A back-flow through the core of this vortex transports fluid to the inlet.

The flow patterns inside the Two-Strand-Tundish can be determined using the PLIF-Method. Figure 4 shows the formation of a mixing area 100 s ($\Theta = 0.17$) after fresh water is delivered into the tundish. The turbulent structure of the entering jet can be clearly seen. The high flow velocities in the inlet region of the tundish lead to intensive mixing effects. The PLIF as well as the DPIV-measurement show that a stagnant region is generated near the surface between $x/B = 0.7$ and the rear wall of the tundish.

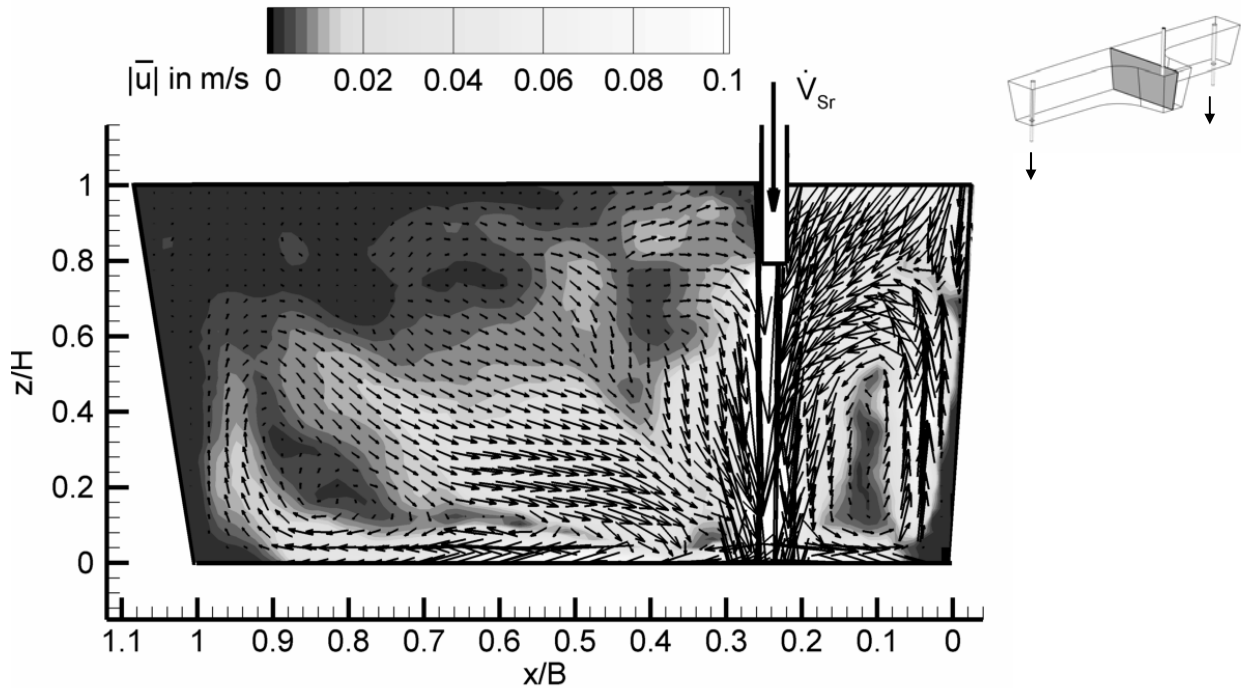


Figure 3: DPIV-Measurement of the isothermal flow field of the Two-Strand-Tundish, symmetry plane

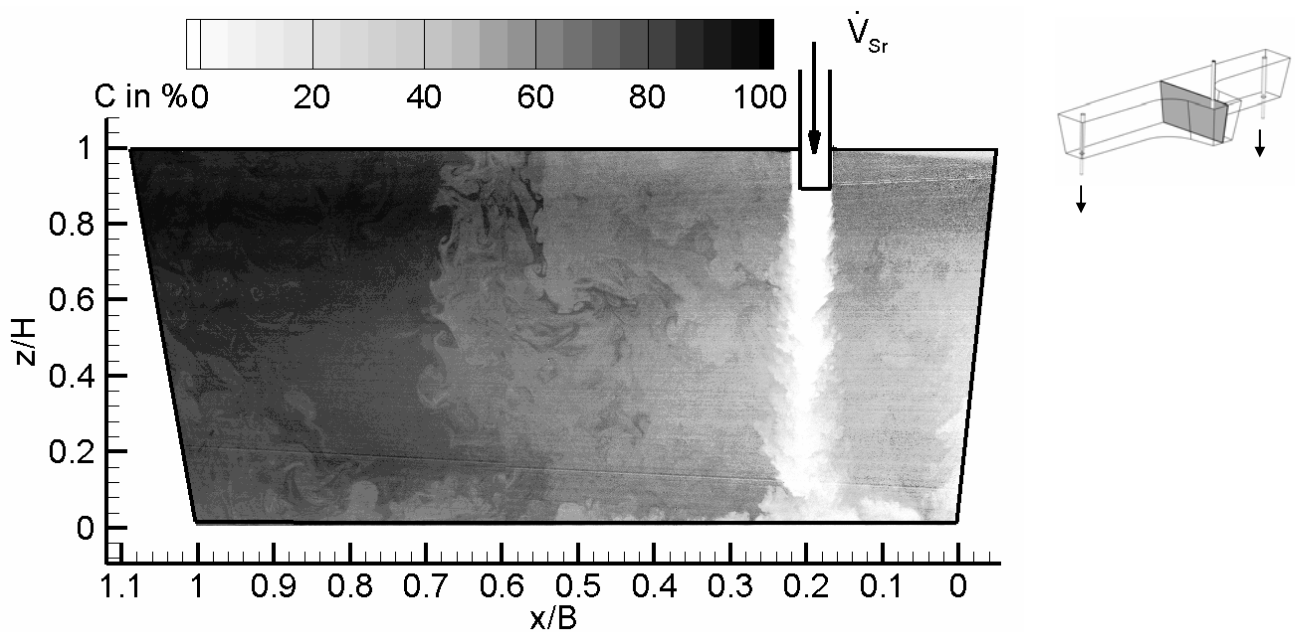


Figure 4: PLIF-Measurement of the isothermal concentration field inside the Two-Strand-Tundish, $\theta = 0.17$, symmetry plane

The progress of the mixing process in the inlet region is illustrated in Figure 5. After $t = 250$ s ($\theta = 0.45$) the maximum concentration of Rhodamine 6G in the inlet region is below 70%, Figure 5. The strong mixing process is induced by the high velocities of the shroud jet. The fresh water hits the rear wall and is redirected in direction to the SEN's.

a)

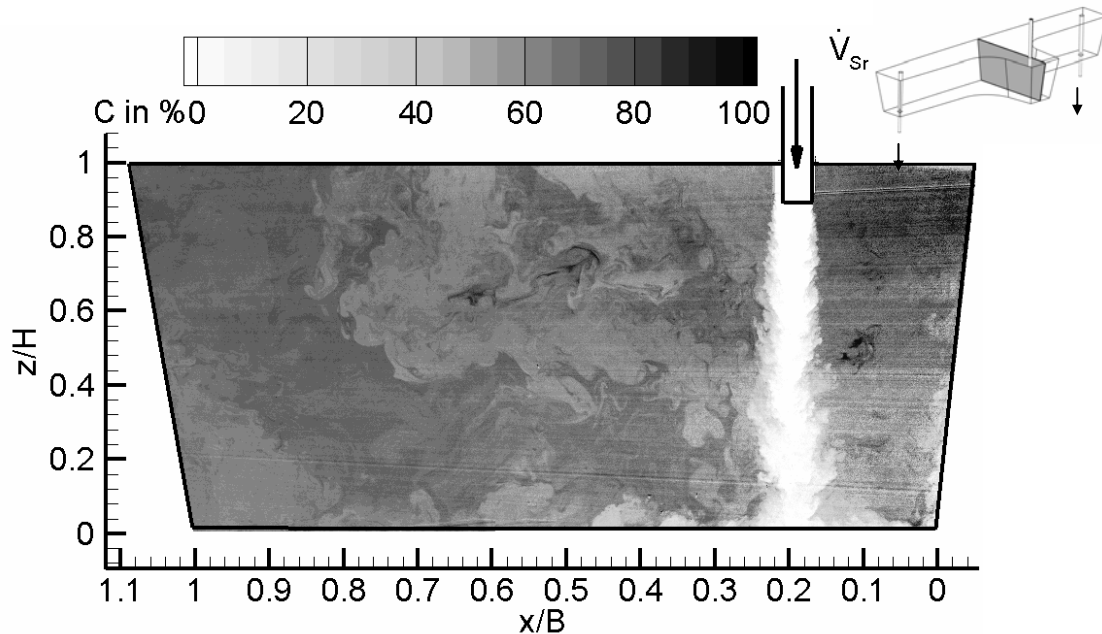
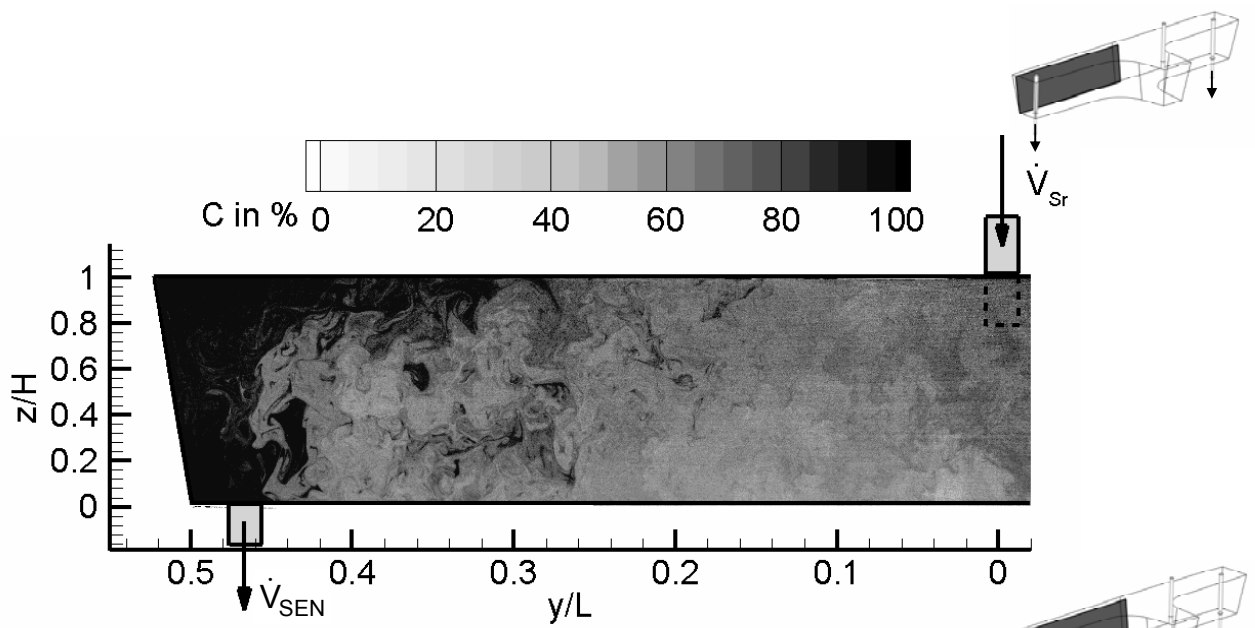


Figure 5: PLIF-Measurement of the isothermal concentration field inside the Two-Strand-Tundish, $\Theta = 0.45$, symmetry plane

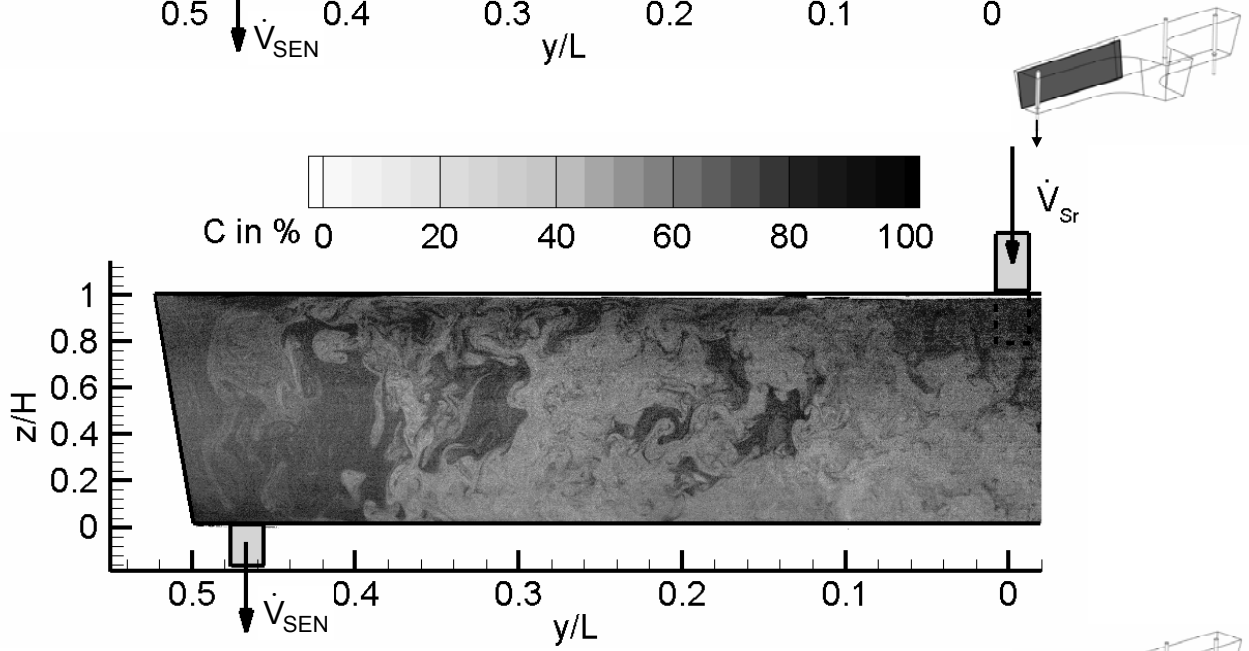
Figure 6 displays the dependency of the mixing progress on the casting conditions. In the case of undisturbed casting conditions a concentration front moves through the outlet region along the rear walls and reaches the SEN after $t = 250$ s ($\Theta = 0.45$), Figure 6a. During a casting disturbance the mixing process in the active side, Figure 6b is similar to the undisturbed casting conditions. The passive side, Figure 6c, shows a strong correlation between the propagation of the concentration field and the casting conditions. The concentration front does not expand into the passive side of the tundish.

This mixing process can also be seen along the side wall. For undisturbed casting conditions, Figure 7a, and for the active side during disturbed casting conditions, Figure 7b, the concentration front moves almost through the complete outlet region. Whereas the fresh water in the passive side does not expand beyond the middle of the outlet region.

It can be concluded that a casting disturbance has a strong influence on the flow field, especially on the tundish-half of the affected mould. A wide-ranging stagnant region develops in this tundish half. Transferred to the casting process, these regions support strong cooling effects. To avoid freezing effects of the melt a premature interruption of the casting process would be necessary.



b)



c)

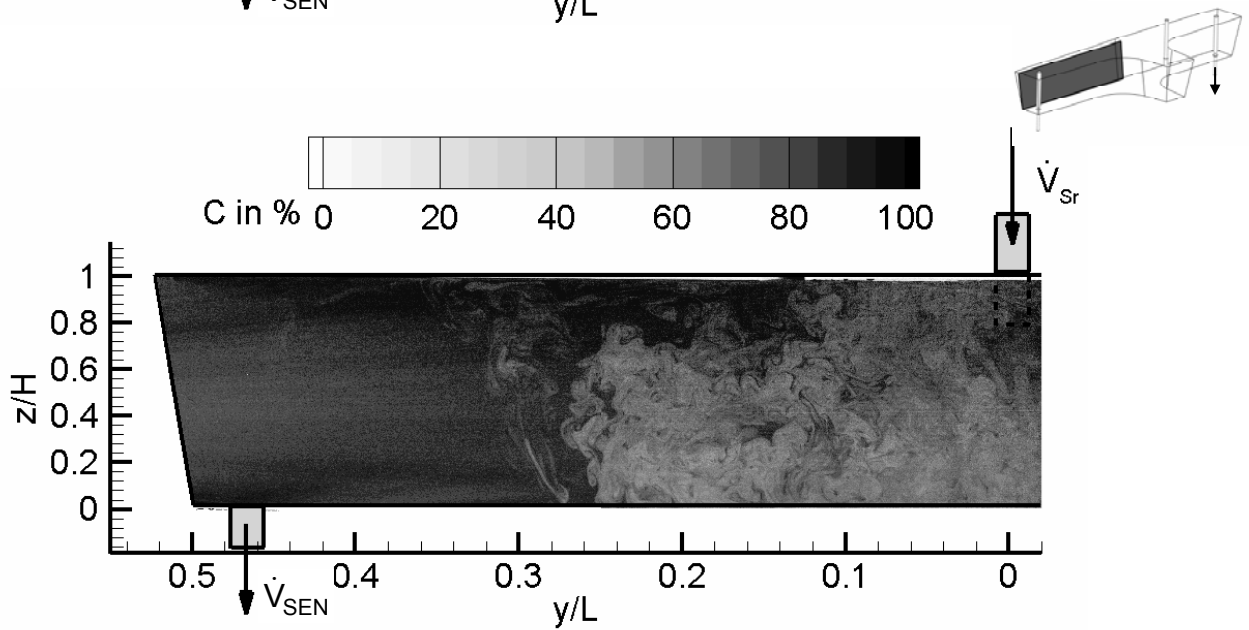
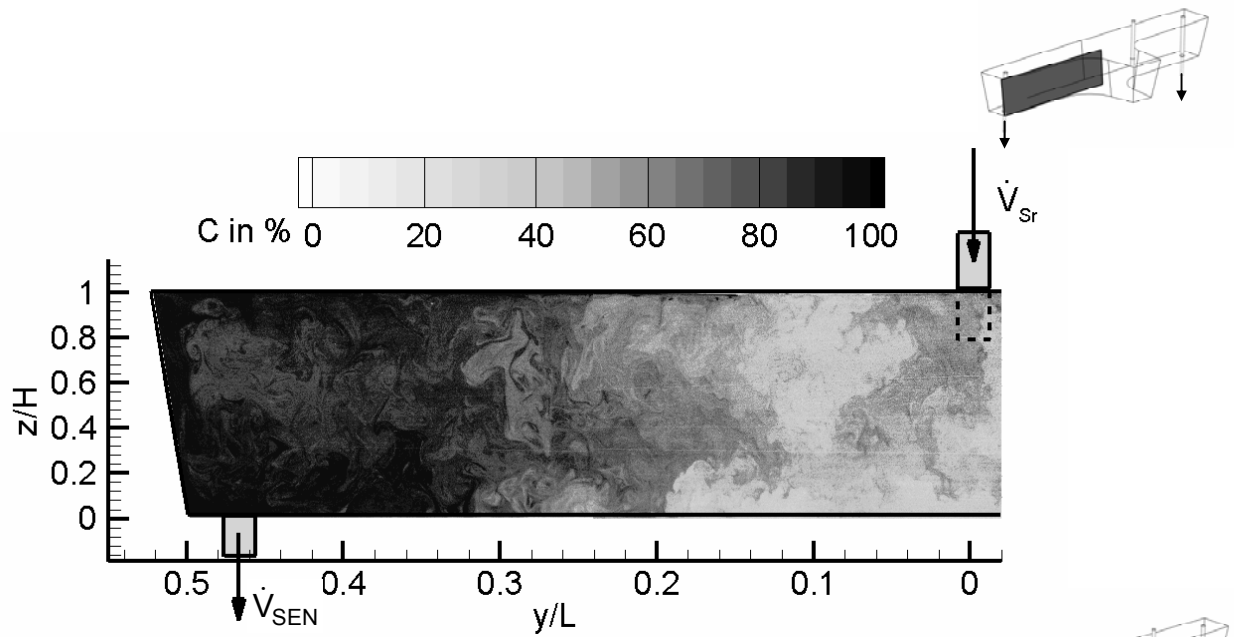
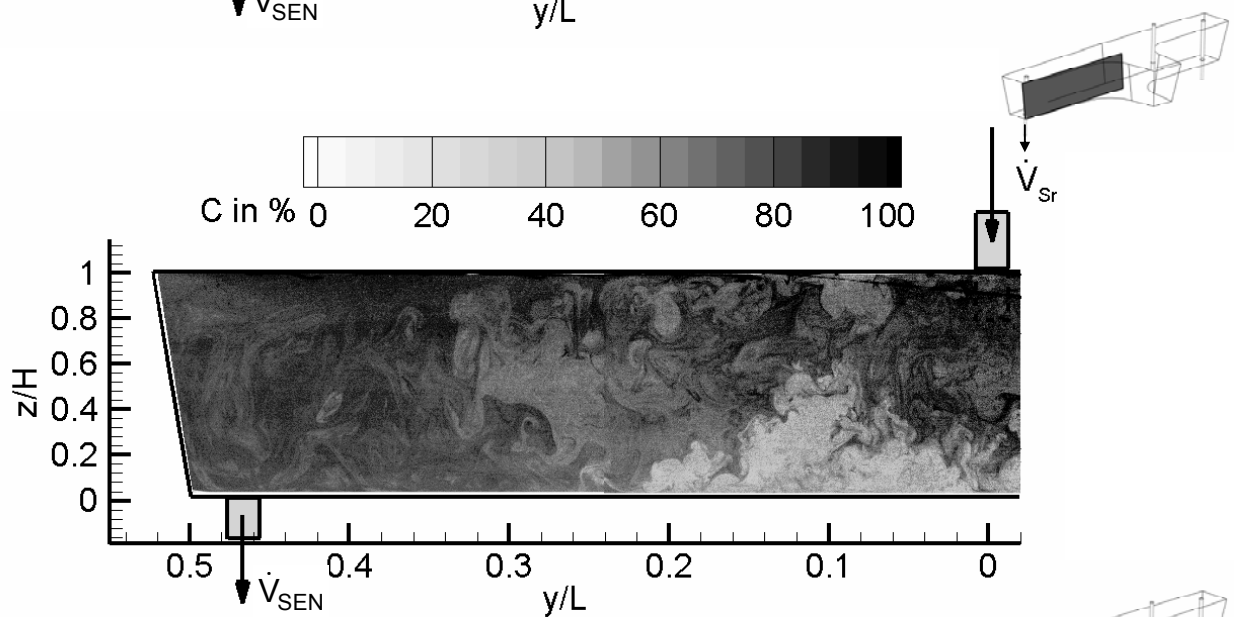


Figure 6: PLIF-Measurement of the isothermal concentration field inside the Two-Strand-Tundish, $\theta = 0.45$, rear wall, a) undisturbed, b) active side, c) passive side

a)



b)



c)

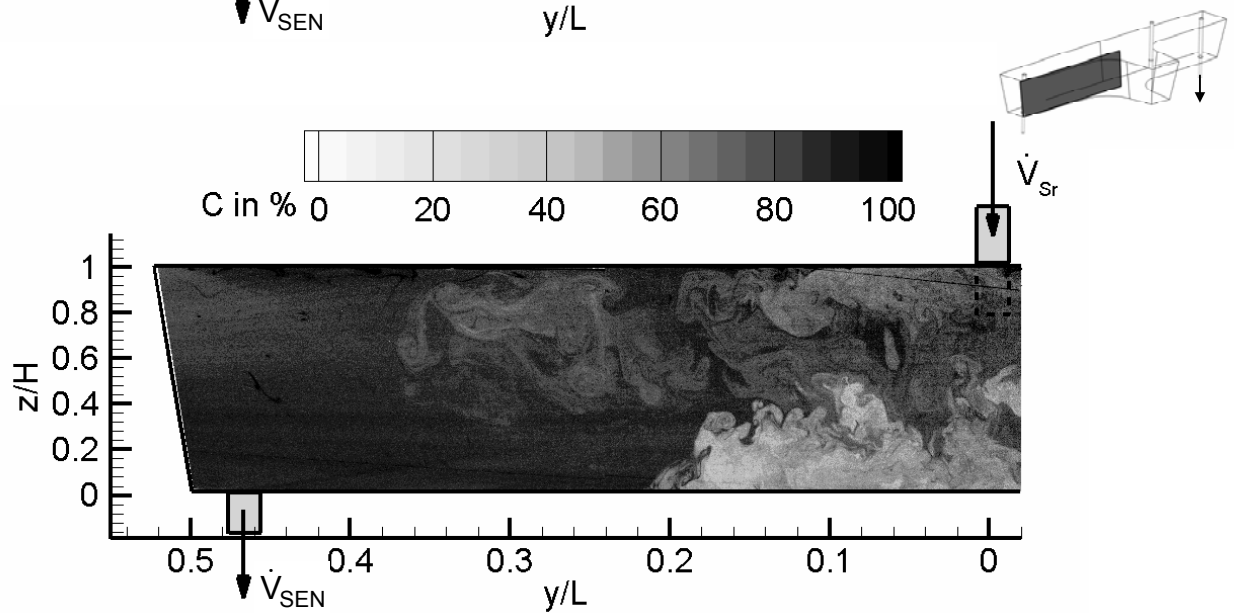


Figure 7: PLIF-Measurement of the isothermal concentration field inside the Two-Strand-Tundish, $\theta = 0.45$, side wall, a) undisturbed, b) active side, c) passive side

ACKNOWLEDGMENT

The authors gratefully acknowledge the financial support of the Deutsche Forschungsgemeinschaft (DFG).

References

- [1] Braun, A., Pfeifer, H.: "DPIV-Messungen der Strömungsstrukturen bei Gießstörungen in einem Zweistrang-Verteiler, 13. Fachtagung, Lasermethoden in der Strömungsmesstechnik, Shaker Verlag, Cottbus, 2005, S12.1-9.
- [2] M.C.J. Coolen, R.N. Kieft, C.C.M. Rindt, A.A. van Steenhoven: *Experiments in Fluids* 27, 1999, No 5, 420-426.
- [3] Damle, C., Sahai, Y.: A criterion for water modeling of non-isothermal melt flows in continuous casting tundishes, *ISIJ International*, Vol. 36, 1996, No. 9, p. 681-688.
- [4] Dantec Dynamics: *Planar-LIF software for Flow Manager - Installation and Users Guide*, 2002.
- [5] Joo, S.; Guthrie, R.I.L.: "Inclusion behaviour and heat-transfer phenomena in steel-making operations: Part I Aqueous modelling", *Met. Trans. B*, Vol. 24B, 1993, p. 755-765.
- [6] Koitzsch, R., Odenthal, H.-J., Pfeifer, H.: "Concentration measurements in a water model tundish using the combined DPIV/PLIF technique", *Steel research*, Vol. 78, 2007, No. 6, p. 473-481.
- [7] Miki, Y; Thomas B.G.: "Modeling of inclusion removal in a tundish", *Met. Trans. B*, Vol. 30B, 1999, p. 639-654.
- [8] Odenthal, H.-J., Bölling, R., Pfeifer, H.: "Analyse dynamischer Strömungsvorgänge im Stranggießverteiler mit Turbostopper mittels LDA, PIV und CFD-Methoden", 9. GALA Fachtagung, Lasermethoden in der Strömungsmesstechnik, Shaker Verlag, Winterthur (CH) 2001, S.40.1-8.
- [9] Odenthal, H.-J.: "Physikalische und numerische Strömungssimulation kontinuierlicher Gießprozesse der Hochtemperaturtechnik", *Habilitationsschrift*, Fachbereich Georesourcen und Materialtechnik, 2004, RWTH Aachen.
- [10] Odenthal, H.-J., Pfeifer, H.: PIV- und LDA-Messungen an Turbostoppfern zur Strömungsoptimierung in Stranggießverteilern, 8. GALA Fachtagung, Lasermethoden in der Strömungsmesstechnik, Shaker Verlag, München, 2000, S. 28.1-7.
- [11] Odenthal, H.-J., Bölling, R., Pfeifer, H.: "Untersuchung instationärer und thermischer Strömungseffekte in Stranggießverteilern", 10. GALA Fachtagung, Lasermethoden in der Strömungsmesstechnik, Shaker Verlag, Rostock, 2002, S.45.1-11.
- [12] Raffel, M., Willert, C., Kompenhans, J.: *Particle image velocimetry – A particle guide*. Springer, 1998.